LAWRENCE
LIVERMORE
NATIONAL
LABORATORY

UCRL-CONF-213672

Statistical Hot Spot Model for Explosive Detonation

A. L. Nichols, III

July 18, 2005

Shock Compression of Condensed Matter
Baltimore, MD, United States
July 31, 2005 through August 5, 2005

STATISTICAL HOT SPOT MODEL FOR EXPLOSIVE DETONATION

Albert L. Nichols III[1]

[1]*Lawrence Livermore National Laboratory, Livermore CA 94551*

Abstract. The Non-local Thermodynamic Equilibrium Statistical Hot Spot Model (NLTE SHS), a new model for explosive detonation, is described. In this model, the formation, ignition, propagation, and extinction of hot spots is explicitly modeled. The equation of state of the explosive mixture is treated with a non-local equilibrium thermodynamic assumption. A methodology for developing the parameters for the model is discussed, and applied to the detonation velocity diameter effect. Examination of these results indicates where future improvements to the model can be made.

Keywords: Detonation**,** hot spots, initiation, failure diameter, shock waves, computer model
PACS: 82.40.Fp, 82.33.Vx, 62.50.+p, 81.05.Lg.

INTRODUCTION

The presence and need for energy localization in the ignition and detonation of high explosives is a corner stone in our understanding of explosive behavior. This energy localization, known as hot spots, provides the match that starts the energetic response that is integral to the detonation.

Processes involved in ignition must be present during detonation, since the shocked material can not distinguish between a shock from a flyer plate or a continuing detonation. The energy deposited in the reactant by the shock process has both uniform and localized contributions. The uniform energy deposition arises from the viscous dissipation of the shock progressing over uniform material. This will heat the material and can potentially cause reaction, if the shock is strong enough. The bulk reactivity can cause the complete decomposition of the explosive with out detonation. However, for many explosives, the shock required to detonate a uniform crystal is stronger than that produced by the detonation of the explosive itself. Thus other mechanisms are needed in order for the detonation to progress. Localized energy deposition, known as a hot spot, arises from a variety of defects in the explosive material. All defects are pre-existing, and can in principle be counted.

In our model, we use the life cycle of a hot spot to predict explosive response. This life cycle begins with a random distribution of potential hot spots. A shock wave either transforms these into hot spots that then grow by consuming the explosive around them or collapses them without causing ignition. In our approach we do not assume that every hot spot is burning in an identical environment, but rather we take a statistical approach to the burning process. We also track the flow of energy from reactant to product, allowing a non-uniform temperature.

NON LOCAL THERMODYNAMIC EQUILIBRIUM STATISTICAL HOT SPOT MODEL

Nichols and Tarver [1] initially described the statistical hot spot formulation. The first phase in constructing the statistical hot spot model is the consideration of the distribution of those hot spots. First, the probability that a single hot spot of radius R will have reacted at a given location in a volume

V in the explosive is simply the volume of the hot spot divided by the total volume. The probability that any given region of space has not been burned is just the product of the probability that it has not been burned by any specific hot spot. Taking the limit where the total volume becomes large but the density of hot spots of size R, ρ(R), remains constant, we have the final expression for P_{nr} :

$$P_{nr} = \exp\left(-\frac{4\pi}{3} \int_0^\infty R^3 \rho(R) dR \right) \tag{1}$$

The probability of not yet reacting is simply the mass fraction of the reactant in a reactive flow formulation. The probabilistic formulation makes it easier to consider a variety of different possibilities. For example, a similar reasoning can be used for two-dimensional hot spots (hotlines) and one-dimensional hot spots (hotplanes). If all of such ignition mechanisms could be defined, all that would be required for a complete hot spot model is to multiply their probability functions together.

We define the probability density of the hot spots as:

$$\rho(R,t) = \rho_A(R,t) + \rho_D(R,t) \tag{2}$$

$$\rho_A(R,t) = \int_{-\infty}^{t} d\alpha \int_t^\infty d\omega \, \rho_s(\alpha,\omega) \delta\left(R - \varepsilon - \int_\alpha^t d\tau v(\tau) \right) \tag{3}$$

$$\rho_D(R,t) = \int_{-\infty}^{t} d\alpha \int_{-\infty}^{t} d\omega \, \rho_s(\alpha,\omega) \delta\left(R - \varepsilon - \int_\alpha^\omega d\tau v(\tau) \right) \tag{4}$$

where $\rho_s(\alpha,\omega)$ is the number density of hot spots that ignited at time α, and died at time ω. The Dirac-delta functions are used to define the size of the hot spot with the assumption that the initial hot spot size is ε, and that it then burns at a burn rate *v* out from that initial spot. The first term $\rho_A(R,t)$ represents the population of hot spots of size R that are still growing (active) at time t. The second term $\rho_D(R,t)$ represents the population of hot spots of size R that have stopped growing (died) by time t. Even though a hot spot may stop burning, the material that has burned within that hot spot must still be counted as reacted.

Let us now define the following projections of the density function:

$$\begin{aligned}
h(t) &= \frac{4\pi}{3} \int_0^\infty dR \, R^3 \rho(R,t) \\
\bar{g}(t) &= \pi \int_0^\infty dR \, R^2 \rho_A(R,t) \\
\bar{f}(t) &= 2 \int_0^\infty dR \, R \rho_A(R,t) \\
\bar{\rho}_A(t) &= \int_{-\infty}^{t} d\alpha \int_t^\infty d\omega \, \rho_s(\alpha,\omega) \\
\rho_B(t) &= \int_t^\infty d\omega \, \rho_s(t,\omega)
\end{aligned} \tag{5}$$

The h term is just the negative of the log of the probability defined in Eq. (1). The number of hot spots that are active at time t is $\bar{\rho}_A(t)$, and ρ_B(t) is the number of hot spots created at time t. In the current model, it is assumed that all active hot spots have the same rate of death μ(t). We can now construct a set of differential equations to couple the high order reactant mass fraction with the much simpler active hot spot density.

$$\begin{aligned}
\frac{\partial h}{\partial t} &= 4v(t)\bar{g}(t) + 4\pi\varepsilon^3 \rho_B(t)/3 \\
\frac{\partial \bar{g}}{\partial t} &= \pi v(t)\bar{f}(t) + 4\pi\varepsilon^2 \rho_B(t) - \mu(t)\bar{g}(t) \\
\frac{\partial \bar{f}}{\partial t} &= 2v(t)\bar{\rho}_A(t) + 2\varepsilon\rho_B(t) - \mu(t)\bar{f}(t) \\
\frac{\partial \bar{\rho}_A}{\partial t} &= \rho_B(t) - \mu(t)\bar{\rho}_A(t)
\end{aligned} \tag{6}$$

Properties of the Hot spot Density Model

It is interesting to note some of the limits associated with the SHS model and compare them with the standard reactive flow models of Tarver. If we assume that the shock promptly ignites the hot spots, then the initial rate of fraction reacted *x* will progress as $\dot{x} \propto x^{2/3}$. This is in accord with most of the reactive flow models. However, at long times, the rate of reaction will progresses as $\dot{x} \propto -(1-x)\ln(1-x)$. Note that this rate expression

cannot be formulated as a power-law, as is the standard scheme in reactive flow rate laws. In fact, the SHS model is slower at finally consuming the reactant than any power law dependence less than 1. On the other hand, a form factor reaction with coefficients 2/3 and 0.7, i.e. $\dot{x} \propto x^{2/3}(1-x)^{7}$, provides a good fit through the peak in the reactivity and is only slightly faster during the completion phase of the reaction.

Ignition model

Next we must define the rate at which hot spots are created. In order to model the explosive process, we choose an ignition model that can encompass a variety of high explosives phenomena. We begin by defining the initial density of potential hot spots ρ_P^0. We currently limit ourselves in that the potential hot spot must transform into a roughly spherical hot spot. Most postulated hot spot formation mechanisms involving void collapse predict that spherical hot spots form upon full collapse[2]. The shock compresses the potential hot spots. The shock must have sufficient power to overwhelm the strength of the explosive to cause internal void collapse. If compressed slowly, the potential hot spot will be destroyed without creating a hot spot, while if compress to sufficiently high temperature, they will start to react. The following phenomenological ignition model captures these features.

$$\mathrm{K}(p) = \left(\frac{A_I P^*(p - P_0)}{P^* + p - P_0} \right) H(p - P_0) \tag{7}$$

$$\begin{aligned} \dot{\rho}_P &= -\rho_P \mathrm{K}(p) \\ \rho_B &= \rho_P (\mathrm{K}(p) - \mathrm{K}(P_A)) H(\mathrm{K}(p) - \mathrm{K}(P_A)) \end{aligned} \tag{8}$$

Here K(p) is the rate of potential hot spot transformation, and $\mathrm{K}(P_A)$ is the constant death rate for potential hot spots. P_0 is the ignition rate threshold pressure that represents the internal resistance to void collapse. To prevent unrealistically large collapse rates during numerical pressure spikes, P^* is defined as the saturation pressure. *H(u)* is the Heaviside step function, which is zero for $u<0$ and one for $u>0$. More complex ignition models can be formulated as this model evolves.

Non-Local Thermodynamic Equilibrium Chemical Material model

We need to define the model for the equation of state of the mixture of reactants and products. In our model, the extent of composition change and the hydrodynamic work are conducted simultaneously and self consistently. At the beginning of a time step, the state of the material is given by the mass fractions $\{x_i\}$, specific energies (energy per reference volume) $\{e_i\}$, and specific relative volumes (volume per reference volume) $\{v_i\}$ of each species i. We also can define the total energy and volume of the system:

$$e = \rho^0 \sum_i e_i x_i / \rho_i^0; \quad v = \rho^0 \sum_i v_i x_i / \rho_i^0 \tag{9}$$

where ρ^0 is the reference density of the chemical material, and ρ_i^0 is the reference density of the i^{th} species. We need to follow the energy of the system through the reactivity, heat and work phases. By defining x_{ij} as the change increase in the mass fraction of the i^{th} species that came from the j^{th} species, we have that the mass fraction change is just the difference between the influx and outflux.

The NLTE chemical material model is solved implicitly, insuring that the extent of reaction and species pressure equilibrium is achieved. Each pass is broken into four phases. The first phase calculates the extent of reaction based on the average of the initial and final pressures and temperatures of the previous pass. For the initial pass, only the initial condition is used. During each of the second and fourth phases half of the change in mass, energy, and volume of each of the species is moved from the reactant to the product. So for the mass, energy, and volume we use the following equation by replacing ξ by ρ_i^0, e, or v:

$$\frac{\xi_i^{II} x_i^{II}}{\rho_i^0} = \frac{\xi_i^t x_i^t}{\rho_i^0} - \frac{1}{2}\sum_j x_{ji} \frac{\xi_i^t}{\rho_i^0} + \frac{1}{2}\sum_j x_{ij} \frac{\xi_j^t}{\rho_j^0} \tag{10}$$

It is important to note that the process from going from state “t” to state “II” (or “III” to

"$t+\Delta t$" in the fourth phase) conserves total mass, volume and energy. It can be thought of separating an appropriate amount of mass with its energy and volume and transferring it to that of the receiving species.

The third phase of each pass changes the volume of each species while holding the composition fixed. This last constraint implies $xi^{II} = xi^{III}$. The energy is updated by a third order Runga-Kutta integration of the pdv work with the addition of an external heat source, ω_i.

We require that the internal energy change calculated by the sum of the species processes be equal to the change of the total internal energy. That implies the following requirement:

$$\begin{aligned} &\omega - \int_{v^t}^{v^{t+\Delta t}} (p+q)dv \\ &= \sum_i \frac{\rho^0}{\rho_i^0} x_i^{II} \omega_i - \sum_i \frac{\rho^0}{\rho_i^0} x_i^{II} \int_{v_i^t}^{v_i^{t+\Delta t}} p_i dv_i \end{aligned} \tag{11}$$

The artificial viscosity q will be divided into two parts: q^e the artificial viscosity derived from the element motion, and q^i that derived from internal processes. In our current model, the assumption is made that the external energy and $q^e dv$ work associated with the zone is distributed equally to each species by their mass.

Once the energy and volume have been calculated for the "$t+\Delta t$" state, we calculate the pressure and temperature using the equation of state for each species. These state variables are used to calculate the reaction rates in phase 1 of the next pass. Note that these phases define the process by which the NLTE chemical element proceeds from its initial state to its final state. We require pressure equilibrium in the NLTE chemical material at the end of the time step to close the thermodynamic relations. This is achieved by using standard Newton-Raphson solution techniques to determining the value of v_j^{III}. for pressure equilibration of $P^{t+\Delta t}$. We simplify the derivative term to its zero reaction limit to reduce the complexity in exchange for requiring smaller time steps.

Finally, to define the internal artificial viscosity q^i we note that p+q at the end of the time step for the entire element needs to be the appropriate sum of those for each component as work was begin performed.

Having described the process for each pass, the code iterates on the v_j^{III} until pressure and reaction equilibration have occurred.

MODEL PARAMETERIZATION

In general, we use the same arguments defined in Nichols and Tarver [1] to define the 8 non-equation of state parameters for the statistical hot spot model: P_0, P^*, A_i, μ, v, P_A, $\rho_P{}^0$, and ε. P_0 is related to the yield strength, and so we use that in our model. The burn velocity v is experimentally determined by any of the standard burn rate measurement techniques, such as strand-burner and diamond anvil experiments. The value of P_A is chosen to match explosive shock recovery experiments. The heuristic arguments for $\rho_P{}^0$, and ε have been modified. If one assumes that the total initial hot spot volume will equal the initial void volume and that enough hot spots need to be created so that when they burn with velocity v at the detonation pressure p_D, they will consume the entire explosive in the reaction zone time τ and initial void density ρ_v, then:

$$\begin{aligned} \rho_v &\approx 4\pi\varepsilon^3 \rho_P^0/3 \\ \rho_A^0 &\approx \rho_P^0[1 - K(P_A)/K(p_D)] \\ 1 &\approx 4\pi(\varepsilon + v\tau)^3 \rho_A^0/3 \end{aligned} \tag{12}$$

Reactant and product equations of state are needed to describe the states attained during shock compression. The Jones-Wilkins-Lee (JWL) equation of state is used for the reactant with typical parameters for an HMX-based plastic bonded explosive.

$$P = A\left(1 - \frac{\omega}{R_1 V}\right)e^{-R_1 V} - B\left(1 - \frac{\omega}{R_{12} V}\right)e^{-R_2 V} + \frac{\omega E}{V} \tag{13}$$

where P is pressure, V is relative volume, E is the internal energy, ω is the Gruneisen coefficient, and A, B, R_1, and R_2 are constants. For a typical HMX-based plastic bonded explosive, the initial density is 1.85 g/cm^3, $R_1 = 14.1$, $R_2 = 1.41$, $\omega = 0.8938$, A = 9522 Mbar, and B = 0.05944 Mbar. This JWL

equation fits the measured reactant Hugoniot data at low shock pressures and the von Neumann spike data at high pressures [3]. The reaction products are described by LEOS tables fit to product equation of state calculated by the CHEETAH chemical equilibrium code[4].

RESULTS

As previously discussed, the ignition and growth of reaction model has eight parameters: P_0, P^*, A, μ, v, P_A, ρ_P^0, and ε. The reaction growth rate v is set to experimentally measured burn rates of pure HMX from the strand burner [5] and diamond anvil cells [6]. The pressure versus burn rate is shown in Fig 1. Two models were developed based on two interpretations of the burn rate data. The following values are used for both models: $P_0 = 0.6$ GPa, $P_A = 1.2$ GPa, $P^* = 10$ GPa, $\rho_v = 0.02$, $\tau = 9\ ns$, and $\mu = 1 \mu s^{-1}$. The first model sets $\varepsilon = 8.64e^{-2}$ μm, $\rho_P^0 = 7.4e^{+12}$ cm^{-3}, $A = 5.2e^4$ cm-μs/g, and D=293.μs^{-1}. P_0 is set to the Hugoniot elastic limit for HMX [7]. P_A has been set to twice the Hugoniot elastic limit. The burn rate pressure exponent of ~0.75 essentially matches the experimental data. The second model uses ε =1.05 μm, ρ_P^0 =4.09e^9 cm^{-3}, A = 4.2e^3 cm-μs/g, D=24. μs^{-1} and follows the higher-pressure burn rate and then continues with an exponent of 2 to the detonation pressure.

We examine the detonation velocity diameter effect with the statistical hot spot model. In order to determine the detonation velocity, two-dimensional axi-symmetric problems at the requisite diameters were created with a length to diameter ratio of 4, and the calculation was run until the shock wave has proceeded through approximately 90% of the length. The cylinder of explosive was given a velocity of 0.1 mm/μs into a wall. We used a mesh resolution of 1000 elements per cm. The detonation front was captured by tracing the location of the maximum pressure in the axial row of elements. The detonation velocity was calculated by a least squares fit to the final eighth of the time steps.

The detonation velocity versus cylinder diameter for both models and the experimental results of A. W. Campbell and Ray Engelke[8] are plotted in Fig 2. Although model 1 reproduces the detonation velocity diameter effect for large diameters, the detonation continues to propagate even at small diameters, contrary to experimental observation. This behavior is typical of all reaction models that use a pressure burn rate exponent of 0.75. The burn rate does not change rapidly enough to cause the classical detonation failure.

One issue that could affect the model is the burn rate function. The experimental data that we use was collected at room temperature. Temperature changes of a thousand degrees should result in significant increases to the burn rate. An effective burn rate with a higher-pressure exponent would represent the temperature increased burn rate since temperature increases with shock pressure. This is the basis of model 2. Model 2

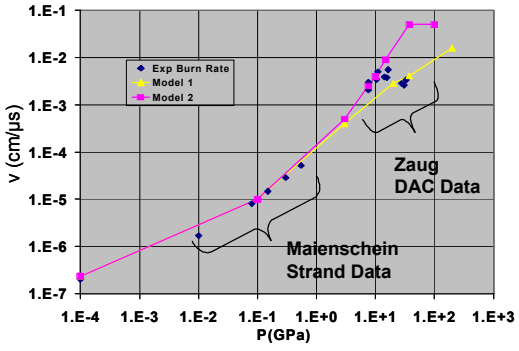

Figure 1. Hot spot burn rate vs. Pressure. The points are the experimental data, the light line is model 1 and the dark line is model 2.

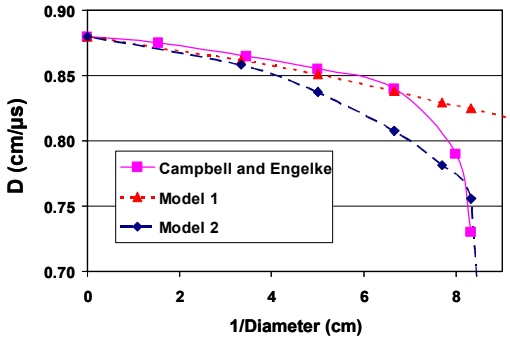

Figure 2. Detonation Velocity as a function of inverse cylinder diameter. The solid square dots are the experimental results of Campbell and Engelke. Model 1 has a explosive burn rate exponent of approximately 0.75, while model two has a higher exponent above 3 GPa.

slightly under predicts the detonation velocity in the intermediate diameters until just before detonation failure. The model does reproduce the classic detonation failure diameter.

The fact that this model does not properly fail at small diameters leads one to believe that there are processes that are not being captured in this model. One such mechanism would be the bulk heating of the explosive by the detonation wave. To test this idea, we augmented the hot spot reaction with thermal reactions based on the reaction rate parameters of Tarver et. al.[9]. For the current equation of state system, the non-linearity of the thermal reaction rated caused the reactants to transform into products at rates substantially higher than needed. Aside from causing a significant reduction in the time step, this mechanism led to significant numerical instabilities due to the non-linearity of the chemistry.

CONCLUSION

In this paper, we have described a new detonation model for HMX. The equations of state models are based on current best practice. The reaction parameters have been based on available reactant experimental data. The mixture equation of state equilibrates the pressure of each species, while tracking the flow of energy as the composition changes from one species to another. This keeps the reactants cold while the products will be hot, in keeping with the physical model. These models were applied to the detonation velocity diameter effect, to good result.

One issue that needs to be addressed is equation of state of the reactant species at shock conditions. The standard schemes for calibrating the EOS of reactants are capable of determining the pressure at shock compression, but the temperature is more difficult. An improved EOS for temperature is necessary to add a bulk reactivity contribution to the detonation model.

Further investigation into the effect of multiple hot spot sizes should be conducted. Small voids would be more difficult to ignite than large voids. Higher shock pressures would ignite significantly more hot spots than lower pressures. This would increase the effective burn rate at high pressure, as there would be more sites to burn the reactant. As was pointed out, a higher-pressure exponent is necessary to reproduce the detonation failure data.

ACKNOWLEDGMENTS

The author would like to thank Craig Tarver, Jack Reaugh, Brad Wallin and Melvin Baer for useful discussions. Jon Maienschein provided data fits for the strand burned data used here, and Joe Zaug provided early access to and analysis of diamond anvil burn results. This work was performed under the auspices of the U.S. Department of Energy by University of California, Lawrence Livermore National Laboratory under Contract W-7405-Eng-48.

REFERENCES:

1. Nichols, A. L., III, and Tarver, C. M., presented at Twelfth International Detonation, San Diego, CA, 2002.
2. Conley, P. A., Benson, D. J., and Howe, P. M., Eleventh International Detonation Symposium, Office of Naval Research ONR 33300-5, Snowmass, CO, 1998, pp. 768-780.
3. Tarver, C. M., Urtiew, P. A., Chidester, S. K., and Green, L. G., Propellants, Explosives, Pyrotechnics 18, 117 (1993).
4. Fried, L., Howard, W. M., and Souers, P. C., presented at Twelfth International Detonation, San Diego, CA, 2002.
5. Maienschein, J. L. and Chandler, J. B., Eleventh International Detonation Symposium, Office of Naval Research ONR 33300-5, Snowmass, CO, 1998, pp. 872-879.
6. Farber, D. L., Zaug, J. M., and Ruddle, C., Shock Compression of Condensed Matter-2001, Furnish, M. D., Thadhani, N. N., and Horie, Y, eds. CP-620, AIP Press, New York, 2002.
7 . Dick, J. J., and Nartunez, A. R., Shock Compression of Condensed Matter-2001, Furnish, M. D., Thadhani, N. N., and Horie, Y, eds. CP-620, AIP Press, New York, 2002, pp 817.
8. A. W. Campbell and Ray Engelke, 6th Symposium (International) on Detonation, White Oak, MD, August 1976
9. Tarver, C. M., Chidester, S. K., and Nichols, A. L. III, 1996, J. Phys. Chem. 100, 5794.